Alignment and calibration methods for the Belle II TOP counter

M. Starič, for the Belle II TOP group

J. Stefan Institute, Ljubljana, Slovenia

Abstract

At the Belle II spectrometer a Time-of-Propagation (TOP) counter is used for particle identification in the barrel region. The Belle II TOP counter consists of sixteen 2.7 m long modules positioned in the space between the central drift chamber and the electromagnetic calorimeter. We discuss the methods for the alignment and calibration of the TOP counter with measured data.

Keywords: TOP counter, alignment, calibration

1. Introduction

The Belle II experiment [1, 2] is a successor of the Belle experiment at KEK, Tsukuba, Japan. The detector is positioned at the upgraded KEKB collider (SuperKEKB) which will operate at a luminosity of $8 \times 10^{35}\mathrm{cm}^{-2}\mathrm{s}^{-1}$, forty times larger than previously. The Belle II spectrometer is the upgraded Belle spectrometer, where the majority of components have been replaced. In order to cope with higher event rates and higher backgrounds new technologies have been developed and employed. One such new technology is the Time-Of-Propagation (TOP) counter, which will be used primarily to identify hadrons in the barrel region.

The TOP counter is a novel type of particle identification device that combines time-of-flight with the Cherenkov ring imaging technique. A single counter module consists of a long quartz plate, within which Cherenkov photons are emitted along the charged particle trajectory and then transported to the plate exit window by means of total internal reflections. The two dimensional information about the Cherenkov ring image is obtained by measuring the time of arrival and the impact position of photons at the quartz plate exit window. The time of arrival is measured relative to the bunch crossing time and thus includes the time-of-flight of the particle.

The Belle II TOP counter has been discussed by several speakers at this workshop [3, 4]. It is made of sixteen modules positioned in the barrel at a radius of 120 cm and covering the polar angles from 32^0 to 120^0. Each module embodies a 2.7 m long quartz optics, two rows of sixteen MCP-PMT's (Hamamatsu R10754) [5] and wave-sampling electronics [6] connected to each MCP-PMT channel that can measure the photon arrival times to a precision of 50 ps (r.m.s).

In this contribution we present the methods for the alignment and calibration of the TOP counter with measured data.

2. Calibration of time base of sampling electronics

Each channel of the IRSX ASIC waveform sampling electronics [6] consists of an analog sampling array of 128 elements whose delay times must be precisely calibrated. The sampling is synchronized with the SuperKEKB accelerator clock; the accelerator clock is divided by 24 to produce the 21.2 MHz synchronization clock (SSTin) for the sampling electronics. Sampling starts at the rising edge of SSTin and proceeds until the next SSTin cycle comes. The delay-locked loop (DLL) circuit ensures that all 128 samples are done within a single SSTin period. The samples are concurrently transferred [1] to the analog storage consisting of 512 groups of 64-sample storage units, that makes the last 11 μs of the sampled waveform available for further processing.

The goal of the calibration is to find sample time differences $\Delta t_i = t_i - t_{i-1}, \quad i = 1, 2, ..., N$, where t_i are sample times, $N = 128$, $t_0 = 0$ and $t_N = T_{\mathrm{sync}}$, and T_{sync} is the SSTin period. The calibration is done by feeding double pulses of a constant time delay ΔT between the first and second pulse into the channel input. In order to cover all N samples the pulse generator frequency is not synchronized with the SSTin clock. The uncalibrated time of each pulse is then determined using linear interpolation between the two samples at the rising edge where the 50% constant fraction transition occurs.

From the measured uncalibrated times of the first and second pulse, t_1 and t_2, respectively, that are expressed in the number of samples with respect to some earlier SSTin cycle, the corresponding sample numbers modulo N and their decimal parts are determined as

$$s_1 = \mathrm{int}(t_1)\%N, \qquad f_1 = t_1 - \mathrm{int}(t_1), \tag{1}$$

$$s_2 = \mathrm{int}(t_2)\%N, \qquad f_2 = t_2 - \mathrm{int}(t_2), \tag{2}$$

where $\%N$ denotes modulo N operation. The equation for a

Email address: marko.staric@ijs.si (M. Starič, for the Belle II TOP group)

[1] The first half of the sampling array is being transferred when the second half is sampling and vice-versa.

single measurement with precision σ_t can be written as

$$\sum_{k=1}^{N} m_k \Delta t_k = \Delta T \pm \sigma_t, \tag{3}$$

where

$$m_k = \begin{cases} 1 - f_1 & k = s_1 \\ 1 & k = (s_1 + 1, \ \ldots \ , s_2 - 1)\%N \\ f_2 & k = s_2 \\ 0 & \text{elsewhere.} \end{cases} \tag{4}$$

χ^2 can be defined as

$$\chi^2 = \sum_i \frac{(\sum_{k=1}^{N} m_k^{(i)} \Delta t_k - \Delta T)^2}{\sigma_{t,i}^2}, \tag{5}$$

where i counts the measured double pulses. By introducing dimensionless variables $x_k \equiv \Delta t_k / \Delta T$ and $\sigma_i \equiv \sigma_{t,i} / \Delta T$ we obtain

$$\chi^2 = \sum_i \frac{(\sum_{k=1}^{N} m_k^{(i)} x_k - 1)^2}{\sigma_i^2}. \tag{6}$$

The minimization of Eq. 6 gives a linear system of N equations of the form $Ax = b$ with symmetric matrix A

$$A_{kj} \quad = \quad A_{jk} = \sum_i \frac{m_k^{(i)} m_j^{(i)}}{\sigma_i^2}, \tag{7}$$

that can be inverted numerically, and

$$b_k \quad = \quad \sum_i \frac{m_k^{(i)}}{\sigma_i^2}. \tag{8}$$

Therefore $x = A^{-1} b$. The unknown ΔT is then determined from $\sum_{k=1}^{N} x_k \Delta T = T_{sync}$ and the unknown sample times are finally calculated with the procedure: $t_0 = 0$, $t_k = t_{k-1} + x_k \Delta T$, $k = 1, 2, ..., N$.

The calibration method was tested with the calibration double-pulse data taken from one of the modules. The results for one of the channels are shown in Fig. 1; the top plot shows the time difference of the two calibration pulses as a function of sample number when using uncalibrated (equidistant) time base, the plot in the middle shows the time difference when using the calibrated time base, and the plot on the bottom shows the calibration curve. The width of the distribution from the middle plot when projected onto the vertical axis is found to be 42 ps (r.m.s).

We also estimated the number of double pulses needed to obtain a calibration precision that would have a negligible impact on the photon time resolution. We divided the measured sample of double pulses into ten sub-samples and then run the calibration procedure on each of them. The width of residuals of the calibration curves with respect to the full sample is found to be 65 ps (r.m.s.) for 4700 double pulses per channel on average. To obtain a three-times better precision that would contribute marginally to the photon time resolution, an order of magnitude more double pulses (e.g. 50 thousands) per channel would be therefore required.

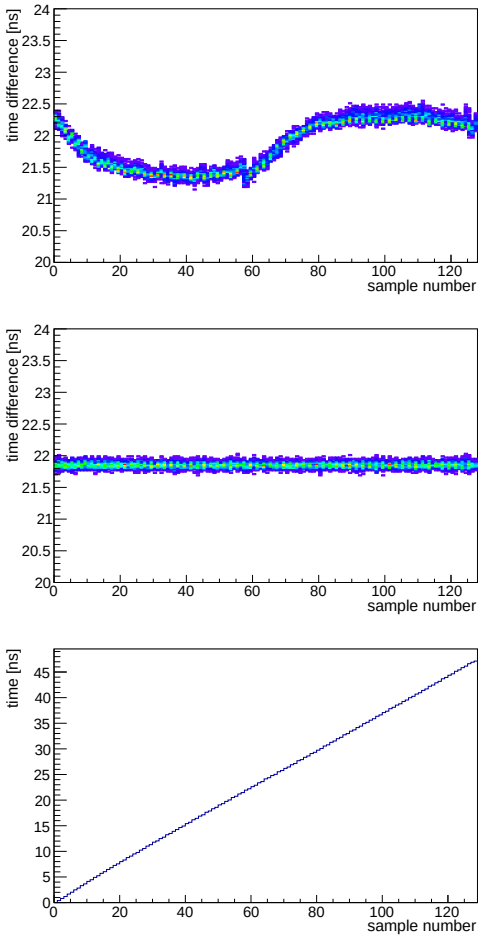

Figure 1: Calibration results for one of the channels. On top: time difference of the two calibration pulses as a function of the sample number, obtained with an equidistant time base. Middle: time difference, when using the calibrated time base. Bottom: calibration curve resulting from time base calibration.

3. Calibration of channel time offsets

The time alignment of channels is done with a laser calibration system [7] incorporated into each module. It consists of a pico-second pulsed laser source coupled to a light distribution system that distributes light to individual modules. The laser output is first split into sixteen single mode optical fibers of equal length that lead the light to the modules. At each module the light is split again into nine, equal length multi-mode optical fibers equipped at output with graded index micro lenses that illuminate the MCP-PMT's from nine positions beneath the slanted prism surface in order to achieve as much as possible a uniform pixel illumination.

The time jitter of the laser pulses is less than 50 ps. However, due to reflections at prism surfaces, a particular MCP-PMT pixel can receive light directly or being reflected once or twice at the prism surface. In addition, some pixels are illuminated with two optical fibers. All these effects result in several different photon arrival times that have to be taken into account.

A simple and robust method can be used for coarse alignment. It relies on aligning the average of measured time distri-

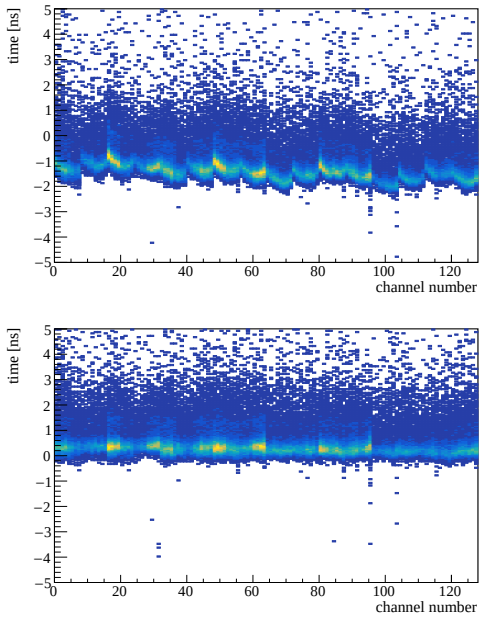

Figure 2: Coarse time alignment of channels using distribution averages; before (top) and after time alignment (bottom). Long tail in time is a nature of TTS.

bution in a pixel with the average of simulated arrival times for that pixel. An example of a coarse alignment with this method is shown in Fig. 2. The drawbacks of this method are hard-to-control systematic biases arising from the differences of simulated and true fiber light emittance.

A refined and more precise method must therefore rely on fitting. The parameterization of the measured distribution in a pixel can be written as

$$f(t) = \sum_k a_k P(t - t_k^{\text{prop}} - t_0), \tag{9}$$

where k counts the different propagation times, a_k are the intensities varying freely in the fit, t_k^{prop} are the propagation times taken from Monte Carlo (MC) simulation and t_0 is the offset to be determined. The distribution $P(t)$ is the time transition spread (TTS) convoluted with the electronic resolution. The TTS was measured with high precision for each channel of every MCP-PMT prior to installation; these data can be used in the fit to reduce the number of free parameters describing $P(t)$. The method is still under development.

4. Alignment of modules

The goal of module alignment is to find small displacements from their nominal position. These displacements can be defined as translations in coordinates x, y and z, $\Delta\vec{r} = (\Delta x, \Delta y, \Delta z)$, and rotations around x, y and z axis by angles α, β and γ, respectively. The transformation of a point at position $\vec{r}$ from the module local frame to the Belle II frame is done in two steps. First we transform the position from local to nominal frame (e.g. displace the module)

$$\vec{r}\,' = R_z(\gamma)R_y(\beta)R_x(\alpha)\vec{r} + \Delta\vec{r}, \tag{10}$$

where R_x, R_y and R_z denote the rotations around x, y and z axis, respectively, and then transform it to the Belle II frame (e.g. position the displaced module to its place in the barrel)

$$\vec{r}\,'' = R_z(\phi)(\vec{r}\,' + \vec{d}), \quad \vec{d} = (0, R, z_0), \tag{11}$$

where R and ϕ are the barrel radius and azimuthal angle, respectively, at which the module is positioned within the Belle II spectrometer, and z_0 measures the displacement in z of the local frame origin with respect to the Belle II origin.

The most suitable data for alignment are di-muon events $e^+e^- \to \mu^+\mu^-$ since they are clean low multiplicity events consisting of two high-momentum particles ($p > 3$ GeV/c) with known particle identity (muons), and whose event rates are comparable to the rates of producing $B\overline{B}$ pairs when running at the energy of $\Upsilon(4S)$.

The alignment parameters can be determined by minimizing the sum of negative log likelihoods over many muons

$$\chi^2(\hat{p}) = -2\sum_{i=1}^{n} \log \mathcal{L}_\mu^{(i)}(\hat{p}), \tag{12}$$

where $\log \mathcal{L}_\mu(\hat{p})$ is calculated with the extended likelihood method using analytic PDF that was discussed at the previous RICH workshops [8, 9], and $\hat{p}$ denotes the vector of alignment parameters $\hat{p} \equiv (\Delta x, \Delta y, \Delta z, \alpha, \beta, \gamma, t_0)$ that must also include the start time offset t_0, since it is correlated with the others.

Minimization of Eq. 12 can be performed with an iterative procedure similar to the Kalman filter. The procedure can be derived in the following way: Suppose we have already minimized Eq. 12 using i muons; we denote the current vector of parameters and the corresponding error matrix as $\hat{p}^{(i)}$ and $V^{(i)}$, respectively. Then, taking the next muon we can write

$$\chi^2(\hat{p}) = -2\log \mathcal{L}_\mu^{(i+1)}(\hat{p}) + \Delta\hat{p}^T V_{(i)}^{-1} \Delta\hat{p}, \tag{13}$$

where $\hat{p} = \hat{p}^{(i)} + \Delta\hat{p}$. The first term in Eq. 13 can be expanded around $\hat{p}^{(i)}$ into a Taylor series up to the second order; then the minimization problem can be solved analytically, resulting in the following iterative procedure:

$$U^{(i+1)} = U^{(i)} - D^{(i)}, \tag{14}$$
$$V^{(i+1)} = [U^{(i+1)}]^{-1}, \tag{15}$$
$$\Delta\hat{p} = V^{(i+1)}\hat{s}^{(i)}, \tag{16}$$
$$\hat{p}^{(i+1)} = \hat{p}^{(i)} + \Delta\hat{p}, \tag{17}$$

where $U = V^{-1}$, $U^{(0)} = 0$, D is a matrix of second derivatives with elements

$$D_{jk} = D_{kj} = \frac{\partial^2 \log \mathcal{L}_\mu}{\partial\hat{p}_j \partial\hat{p}_k} \tag{18}$$

and $\hat{s}$ is a vector of first derivatives with elements

$$\hat{s}_j = \frac{\partial \log \mathcal{L}_\mu}{\partial\hat{p}_j}. \tag{19}$$

The first and second derivatives are calculated numerically at each iteration step.

The alignment method was tested with MC simulation. We generated eight different module displacements and run the

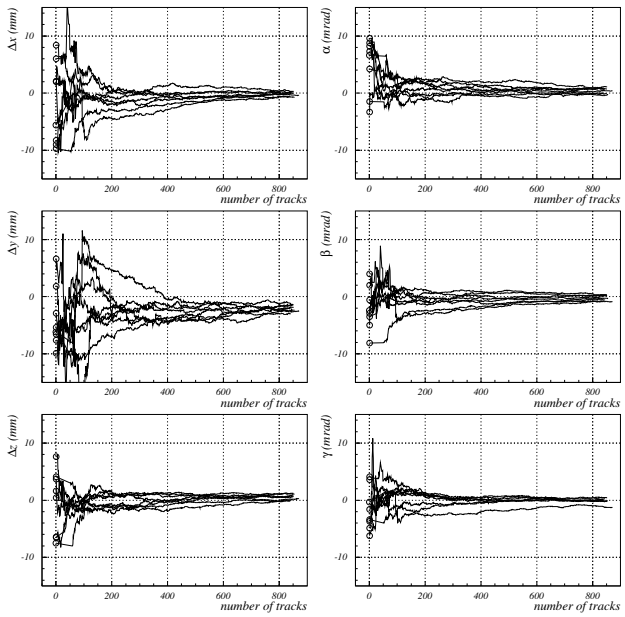

Figure 3: Convergence test of the alignment method with MC simulation. The plots show residuals with respect to the module displacements as a function of the number of muons (iterations). Each curve is for a particular module displacement.

alignment procedure on each of the data sets. In all cases the iterative procedure converges, as shown in Fig. 3. Small biases in y and z that can be noticed in Fig. 3 are under investigation. As expected, the precision scales as $\sigma = \frac{\sigma_0}{\sqrt{n}}$, where n is the number of muons (iterations). The parameter σ_0 is found to be 14 mm for x, 22 mm for y, 12 mm for z, 10 mrad for α, β and γ, and 75 ps for t_0. With a sample of 10000 muons we can align a single module to spatial and angular precisions of 0.2 mm and 0.1 mrad, respectively. These are well below the uncertainties of the tracks extrapolated to the TOP counter.

5. Calibration of the start time offset

As discussed in the introduction, the photon arrival times are measured relative to the bunch crossing time that is given by the accelerator RF clock with some arbitrary offset T_0. This offset has to be determined from data. According to experience from the Belle experiment, slow drifts with time and sudden jumps can be expected, so the offset must be constantly monitored and accounted for.

The method again relies on di-muon events and uses extended log likelihoods calculated with analytic PDF [8, 9]. In this case we search for the minimum of

$$\chi^2(T_0) = -2 \sum_{i=1}^{N} [\log \mathcal{L}^{(i)}_{\mu^+}(T_0) + \log \mathcal{L}^{(i)}_{\mu^-}(T_0)], \qquad (20)$$

where we sum over N di-muon events.

The minimum of Eq. 20 is searched by scanning a selected region of T_0, because local minima are sometimes present. Usually, the scan is done in the region of ± 1 ns around the expected minimum using 200 equidistant steps. The precise position of the minimum is finally obtained by fitting a parabola to the three lowest points.

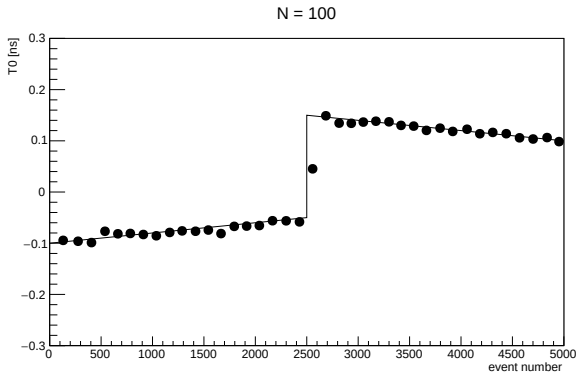

Figure 4: Monte Carlo proof of the principle of T_0 offset monitoring in real time. The solid curve represents the generated offsets slowly drifting with time and with a sudden jump at event number 2500. The points represent the reconstructed offsets. We used 100 di-muon events per point.

The precision for $N = 1$ is found to be about 50 ps; therefore about 100 di-muon events are sufficient to reach the precision of ∼5 ps. The procedure is fast enough to monitor offset T_0 continuously, in time stamps of seconds to minutes. A Monte Carlo proof of the principle is shown in Fig. 4.

6. Conclusions

We discussed the methods for alignment and time calibration of the Belle II TOP counter. The alignment and calibration of the counter need to be performed in the order as presented in this contribution. As the first step the time base of sampling electronics is calibrated using double pulses. Then the time alignment of channels is performed using a laser calibration system. Since a good time resolution is crucial for this kind of detector, these two steps are planned to be repeated on a daily basis. The alignment of the detector with di-muon data is planned after each longer shut-down of the experiment or stronger earth quake that could move the detector structure. Finally, the start time offset calibration can be performed continuously, either during data taking or immediately after it.

References

[1] http://belle2.kek.jp/
[2] T. Abe et.al., KEK Report 2010-1 (2010).
[3] J. Fast, these proceedings.
[4] K. Suzuki, these proceedings.
[5] K. Matsuoka, these proceedings.
[6] G. Varner, M. Andrew, L. Macchiarulo, K. Nishimura, L. Wood, The IRSX ASIC for the Belle II Imaging Time of Propagation Detector, IEEE NSS conference 2015, San Diego, CA
[7] U. Tamponi, these proceedings.
[8] M. Starič et.al., Nucl. Instr. and Meth. A 595 (2008) 252.
[9] M. Starič, Nucl. Instr. and Meth. A 639 (2011) 252.